

Polymerization and Network Formation of UV-Curable Systems Monitored by Hyphenated Real-Time Dynamic Mechanical Analysis and Near-Infrared Spectroscopy

Paul A. M. Steeman, Aylvin A. Dias,* Dietrich Wienke, and Theo Zwartkruis

DSM Research, P.O. Box 18, 6160 MD Geleen, The Netherlands

Received March 31, 2004; Revised Manuscript Received May 26, 2004

ABSTRACT: Hyphenated rapid real-time dynamic mechanical analysis (RT-DMA) and time-resolved near-infrared spectroscopy (RT-NIRS) have allowed simultaneous monitoring of acrylate photopolymerizations with regard to both their chemical conversion and mechanical properties. Up to 374 NIR spectra and up to 50 DMA data points can be accumulated within a second. We observe that modulus buildup does not linearly follow chemical conversion of acrylate bonds. The gel point is detected after passing a certain critical acrylate conversion. Beyond the gel point (determined when the phase angle drops below 45°) network formation proceeds exponentially with acrylate conversion. Experimental data reveal a critical dependence of the mechanical property development during the later stage of acrylate conversion. The experimental results across the modulus–conversion plot reveal the importance of final acrylate bond conversion as opposed to the early part of the conversion vs time (maximum rate of polymerization R_p) when considering the rate of development of mechanical properties (cure speed).

Introduction

Cross-linking photopolymerization reactions are used in performance coatings and composites. The resultant products are used in a wide variety of applications from inks and coatings for optical fibers and food packaging to rapid prototyping (stereolithography) and medical applications such as dental cements and contact lenses. The sophisticated applications found for photocurable systems like optical, medical, and electronic materials have necessitated a better understanding of molecular network structure and the evolution of target mechanical properties.

These photopolymerizations are typically carried out from subsecond to minute time scales. In pursuit of improved control over the development of mechanical properties, techniques that allow the measurement of chemical and mechanical changes in real time or pseudo real time have gained importance. Initially, time-resolved techniques to monitor these fast polymerizations were spectroscopic (real time infrared, RT-IR)¹ and calorimetric (photo-differential scanning calorimetry, DPC). Spectroscopic time-resolved experiments were further improved with the development of Fourier transform instruments that allowed multiple peak monitoring of different reactive chemical groups.² Furthermore, time-resolved spectroscopy of the photocuring reactions also extended to near-IR³ and Raman spectroscopy.⁴ However, these techniques focus on chemical changes and do not give information directly about the development of mechanical properties (extent and density of cross-links.)

Rolla et al. used microwave dielectric measurements to examine the cross-linking polymerization of monofunctional *n*-butyl acrylate⁵ as well as 50/50 w/w blends with a difunctional hexane–diol diacrylate that gave highly cross-linked networks.⁶ In these real time cure experiments the decreasing acrylate monomer concentration was monitored via a linear correlation with the

dielectric loss index at microwave frequencies. This correlation is a result of the largely different time scales for dipolar polarization in the monomer on one hand and in the polymerized reaction product on the other hand. This allowed a detailed study of the reaction kinetics of these acrylate systems.^{5,6}

Direct time-resolved measurement of mechanical properties was initially developed using an oscillating plate rheometer fitted with a quartz parallel plate system.^{7,8} Upon UV irradiation, the dynamic viscosity of these photocurable compositions was seen to increase via the changes in the phase angle and amplitude of oscillation. However, measurements were limited to films/coatings of approximately 10 μm thickness. The added risk of two plates grinding against one another with high shrinkage compositions also means that care has to be taken to ensure that the two plates are indeed parallel. Guthrie et al. compared cone and plate vs the parallel plate geometry in a rheometer modified with a quartz plate. The parallel plate geometry was chosen due to practical considerations and then used to monitor cationic and free radical photopolymerization including pigmented photocurable systems.⁹

Bargon et al.¹⁰ developed a rheological method to monitor laser-initiated photocuring reactions with a quartz microbalance. However, the flow cell experimental setup is of limited utility in coatings or thin films.

Khan and co-workers¹¹ developed real time Fourier transform mechanical spectroscopy (RT-FTMS) during cure by fitting a rheometer with quartz glass plates that allowed one to monitor the evolution of rheological mechanical properties in a temperature-controlled cell. This technique was used to monitor thiol–ene step growth photo-cross-linking polymerization. Just as RT-FTIR instruments allow multiple peak analysis in a single experiment, so-called multiwave or Fourier transform mechanical spectroscopy allows the simultaneous monitoring of rheological properties (dynamic moduli) at several frequencies. This enabled Khan to apply the Winter–Chambon criterion and show that the loss

* Corresponding author: e-mail aylvin.dias@dsm.com.

tangent ($\tan \delta$) becomes independent of frequency at the gel point. RT-FTMS was used to demonstrate for thiolene photopolymerization (tri- and tetrafunctional thiols copolymerized with triallyl isocyanurate) that the cross-linking rate increases by increasing the monomer (thiol) functionality or the temperature. In addition, upon comparing a tri- and tetrafunctional thiol at the gel point, the trifunctional thiol gave stiffer gels than the tetrafunctional thiol. This was attributed to the higher thiol conversions at the gel point for the trifunctional thiol composition.

In a further attempt to understand the relationship between thiol conversion and mechanical properties, Khan and co-workers performed separate RT-FTIR and RT-FTMS experiments using the same light intensity and film thickness.¹² The thiol reactive group was monitored using the S–H vibrational stretch at 2570 cm^{-1} . RT-FTIR studies revealed that the thiol–ene polymerization follows a second-order polymerization until about 70% conversion. RT-FTMS measurements, under identical UV illumination conditions, revealed that the modulus did not change significantly until 65% thiol conversion (according to Flory–Stockmayer manipulation of mechanical data). Thus, comparable gel times were found from both time-resolved IR measurements and time-resolved mechanical analysis.

Acknowledging the utility of both techniques, we introduce a hyphenated time-resolved technique that allows the measurement of reactive group conversion (polymerization) while simultaneously monitoring network formation by the development of mechanical properties with real time dynamic mechanical analysis–near-infrared spectroscopy (RT-DMA/NIRS).

The need to understand the relationship between mechanical properties and chemical reactive group conversion has driven not only technique development but also the development of models to describe network formation in cross-linking polymerizations. Three different modeling approaches have been identified. First, the statistical methods that started with Flory¹³ and Stockmayer^{14,15} have been elaborated by e.g. Gordon,¹⁶ Miller–Macosko,¹⁷ and Durand–Bruneau.¹⁸ Second, kinetic approaches have been developed by e.g. Tobita–Hamielec¹⁹ and Mikos et al.²⁰ Finally, kinetic gelation/percolation type methods have been explored extensively by e.g. Boots et al.²¹ and Bowman.²² The different approaches each have their advantages and limitations. In this paper we use the ability to monitor mechanical properties and chemical conversion to understand in the simplest manner network formation in terms of the gel point and required chemical conversion. As such, the hyphenated RT-DMA/NIRS technique provides a suitable test bed for future evaluation of the various model approaches described in the literature.

Experimental Section

Real Time Dynamic Mechanical Analysis (RT-DMA).

A Rheometric Scientific RDA-2 dynamic analyzer equipped with a 200/2000 g cm dual range torque transducer was chosen for the real time dynamic mechanical analysis setup. In the standard time-sweep measurement mode this instrument can perform dynamic measurements (modulus and phase angle) as a function of time with a single angular frequency. When a high measurement frequency is selected, the instrument can acquire at most one data point per second. Moreover, the standard steel parallel plate assembly does not allow for UV illumination of the sample, nor a diagnostic infrared beam to monitor chemical changes. Therefore, we developed a RT-DMA

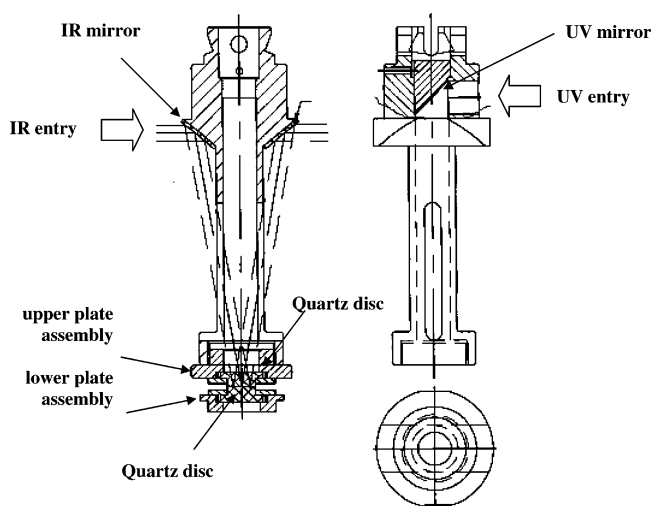


Figure 1. Schematic drawing with front and side view of the DMA/UV/IR upper parallel plate holder fitted with a quartz window and the lower parallel plate assembly. This assembly allows simultaneous illumination of the sandwiched sample between the plates with UV light and a diagnostic near-IR beam.

setup, starting for the design in the original work by Khan and Chiou,¹¹ with the following additional features: (i) a quartz parallel plate geometry that allows both UV and IR penetration; (ii) a high-speed data acquisition utility, able to acquire at least 50 data points per second; and (iii) synchronization between the start of rheometer measurements, UV illumination, and acquisition of infrared spectra.

Two 5 mm thick quartz disks were used as the optically transparent parallel plate measurement system. Quartz is used because it is transparent to both UV light and near-IR. The top half of each disk was machined to a diameter of 12.5 mm and the bottom half to a diameter of 9.5 mm. A metal ring with an opening of 9.5 mm was used to clamp the quartz disk into the plate assembly (see Figure 1). The lower plate assembly was mounted into the standard Rheometric Scientific removable plate holder. Figure 1 shows a front and side view of the new DMA/UV/IR upper plate holder and the lower plate assembly. The upper plate holder comprises an aperture for UV light at the top. UV light is reflected by an internal mirror mounted at an angle of 45° in the center of the plate holder shaft. Two additional external mirrors are mounted at the top of the plate holder, with an entry angle slightly greater than 45°. These provide an optical pathway for an infrared beam. The entry mirror reflects the near-IR light through a side opening in the plate holder shaft to the quartz plates. The bottom of the lower quartz plate is gold-plated and reflects the near-IR beam to the exit IR mirror. The UV-curable material is loaded as a 100 μm thick layer between the upper and the lower quartz disk. The maximum torque of the transducer, in combination with the plate diameter and the sample thickness, limits the shear modulus of the cured sample to a maximum value of about 10 MPa.

Standard time sweeps with the rheometer control software Orchestrator enable a limited data acquisition rate of up to 1 data point per second. Faster measurements can be performed in the so-called arbitrary wave test mode. A user-programmable strain function (vs time) is applied to the sample, while stress and strain data are sampled as a function of time with an acquisition rate up to 160 data points per second. In total, 1600 data points, four blocks of 400 points each, can be sampled in the arbitrary wave mode. The minimum time interval per block is about 2.5 s.

To perform the photocuring measurements, we programmed a sinusoidal strain wave with (strain) amplitude of 10%. Subsequent data analysis was performed with discrete Fourier analysis of the stress and strain signals, a standard feature in the Rheometric Scientific Orchestrator software package. To allow adequate analysis, the sampling rate has to be chosen

such that an integer number of data points are sampled per period of the sinusoidal deformation. In our experiments we programmed a sine wave with a frequency of 8.333 Hz and set the total data acquisition time to 64 s. These settings result in sampling three data points per cycle over 533 periods. The discrete Fourier transform algorithm calculates the magnitude and phase of the stress and strain signals. The dynamic modulus can be calculated by taking the ratio of the stress and strain amplitude, while the phase angle is obtained from the phase shift between these two signals. The phase angle needs a correction for the instrumental phase angle, which is 18.3° in our instrument at the chosen measurement frequency.

Following work by Khan and Chiou,¹¹ we considered the possibility of applying a multifrequency arbitrary wave containing higher harmonics of our 8.333 Hz fundamental frequency. This would enable simultaneous measurements at various frequencies and determination of the gel point according to the Winter–Chambon criterion. However, because of the limited frequency range that the rheometer can apply, we came to the conclusion that this would be possible with the second harmonic only. Moreover, to limit the maximum deformation applied to the sample, it would be necessary to reduce the magnitude of the fundamental wave, which would have a negative effect on the signal-to-noise ratio. Because of these limitations, we decided to perform the experiments at a single frequency only. The consequence of this is that it is not possible to determine the gel times according to the Winter–Chambon criterion, nor are we able to determine the mechanical properties at the gel point instead we use the alternative definition at a phase angle of 45° to identify the gel point.

A Bluepoint-2 lab UV (dr. Hönle GmbH, Germany) source with a F-type bulb was selected for the experiments. An 8 mm diameter liquid light guide was used to guide the UV light from the source to the light entry of the upper plate holder in the rheometer. The intensity (irradiance) of the UV light was measured below the upper quartz plate (prior to loading the sample) with a Solascope-1 radiometer (Solatell, UK). An irradiance of about 28 mW/cm² was detected.

Upon starting the DMA measurement, the control computer downloads the arbitrary wave function into the rheometer for several seconds. At the start of the actual measurement, the “measure in progress” indicator of the instrument is set. We have used this signal to trigger a sequence of events via an external switch box. At the moment that the “measure in progress” signal is set, the switch box triggers the IR spectrometer to start spectrum acquisition. At the same time a delay timer is started which introduces a fixed delay time of 1.575 s before a trigger is sent to the shutter in the UV source. During the delay time both the rheological properties and IR spectra of the uncured liquid resin are monitored. This cascade of automatic triggers greatly simplifies the experiment practically.

Real-Time Near-Infrared Spectroscopy (RT-NIRS). A custom-made NIR diode array spectrometer Milaspec 2000 (producer Polytec-IKS, Tönnisvoort/Germany), equipped with a Peltier-cooled 256 element extended indium gallium arsenide (InGaAs) diode array detector (Sensor Unlimited), was used for the experiments. A fixed grating (Horiba Jobin Yvon) refracts the NIR light onto the diode array. Extended InGaAs detectors can be used to detect NIR in the spectral region between 1200 and 2200 nm with sufficient sensitivity. Thus, overtones and combination vibrations from the acrylate groups can be monitored. One of the overtone absorption peaks is found between 1610 and 1640 nm, depending on the exact type of reactive resin or blend used. The instrument is able to collect up to 500 spectra/s simultaneously through a PCI interface to the data recorder (MS-Windows PC, GRAMS software version 6.0). Sampling frequencies up to 1 MHz per diode are possible. However, a sampling rate of 500 spectra/s seems to be the upper physical limit to get a sufficient number of photons for a reasonable signal-to-noise ratio. The electronics overhead time of 2 ms per spectrum further limits the maximum sampling rate to 374 full NIR spectra/s.

A 50 W halogen lamp is used as an internal NIR light source. The light from the NIR source is guided via a 1 m

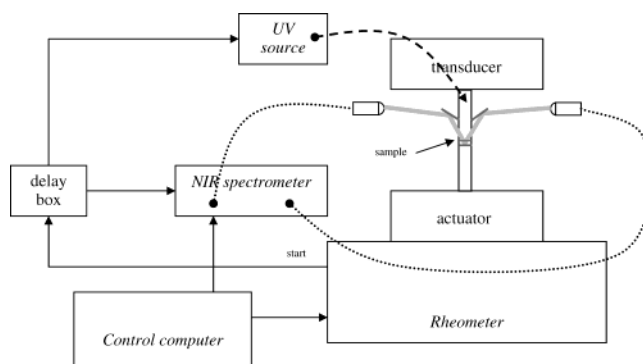


Figure 2. Schematic drawing of the RT-DMA/NIRS setup. A control computer triggers both the DMA and near-IR spectrometer prior to triggering the shutter on the UV lamp.

quartz fiber-optic system to the DMA plate holder. At the end of the fiber a lens that converts the light into a parallel beam is mounted. This parallel beam with a diameter of about 5 mm is directed toward the DMA plate holder IR entry mirror (Figure 1). Next to the DMA plate holder IR beam exit mirror a second lens is mounted to collect the NIR beam and focus it into another quartz fiber that guides the light back to the detector input of the NIR spectrometer. A schematic drawing of the total measurement setup, including the DMA plate holders, the NIR optics from the side, and the UV light guide in front, is shown in Figure 2.

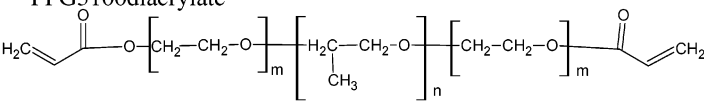
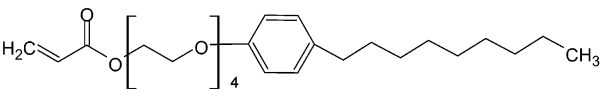
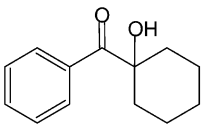
Each experiment starts with the collection of the dark spectrum of the diode array. Next, the reference spectrum is obtained by accumulating 1000 spectra through the total optical path through the RT-DMA instrument without sample loaded. This is to eliminate the spectral characteristics of the gold mirrors, quartz windows, and fiber optics. After this procedure, the instrument is ready for the cure experiment. The total measurement time per cure experiment ranges typically between 10 and 30 s. This results in typical data set sizes of 3500–10 000 full NIR spectra per sample. Dedicated modules written in Galactic GRAMS/6 are used to extract the height of the acrylate absorption peak vs time from this huge number of spectra. Net peak height has been obtained via a piecewise linear baseline fit between 1600 and 1650 nm using dense distributed fit points (GRAMS 6.0 standard algorithm). The intensity of the NIR peak was determined by measuring peak height using the trough method as described by Decker et al.¹ using RT-IR. To obtain better accuracy, before and after the photopolymerization experiment, 3000 dark and background spectra were acquired. This allowed for improved signal-to-noise in the resultant accumulated reference spectra and enables more accurate determination on the absolute levels of conversion. The error is approximately ±2% for this formulation and can be formulation dependent. Finally, the cure profiles are transferred to MS-Excel for further evaluation.

Materials, Synthesis, and Formulations. Synthesis of Ethoxylated Polypropylene Glycol Diacrylate (PPG3100 Diacrylate). Ethylene glycol-terminated polypropylene glycol ($M_n = 3100$ g/mol) (Poly-G polyol 55-37) was obtained from Arch Chemicals. Acryloyl chloride and triethylamine were obtained from Aldrich. Tetrahydrofuran (THF) and toluene were obtained from Merck. Ethoxylated nonylphenolacrylate (SR504) was obtained from Sartomer, and 2-hydroxycyclohexylphenyl ketone photoinitiator (Irgacure 184) was obtained from Ciba-Geigy.

NMR experiments were performed on a Bruker Avance 300 instrument. Non-time-resolved IR measurements were performed on a Perkin-Elmer Spectrum One by applying the neat oligomer as a thin film on NaCl disk. GPC measurements were performed on a Waters system fitted with RI detector (Waters 2410) and UV detector (Waters 2487) set at 254 nm and Styragel HR 0.5-4.0 columns.

29.82 g of PolyG 55-37 diol (M_n 3100) was dissolved in 300 mL of THF in a three-necked round-bottom flask and cooled

Table 1. Acrylate Formulation Based on the Difunctional Telechelic PPG Oligomer of $M_n = 3300$ g/mol and a Monofunctional Ethoxylated Nonylphenol Acrylate

Component	% (w/w)
PPG3100diacrylate  $m = \text{PEG } 22 \text{ w/w} ; n = \text{PPG } 58 \text{ w/w}$	49.0
Ethoxylated nonylphenol acrylate 	49.0
Hydroxycyclohexylphenyl ketone 	1.0
Total	100.0

to 5 °C. To this solution, acryloyl chloride (2 g, 22 mmol) and triethylamine (2.35 g, 23 mmol) were added both as 50 mL THF solutions over a period of 2 h while ensuring that the temperature does not rise above 23 °C. The addition is accompanied by formation of Et_3NHCl precipitate. This precipitate was filtered and a further addition of acryloyl chloride (1 g, 11 mmol) and triethylamine (9.9 mmol) under the same conditions as mentioned earlier. The reaction was left to react for a further 8 h, allowing the reaction mixture to warm to room temperature. The reaction mixture was then cooled to 0 °C and filtered. 0.01 g of hydroquinone was then added to the THF solution, which was then concentrated under reduced pressure and redissolved in toluene. Trace amounts of Et_3NHCl were then removed by filtration followed by evaporation of the toluene under reduced pressure to give 30 g (81% yield) of clear oil that was characterized by ^1H NMR, IR, and GPC.

^1H NMR (CDCl_3 , 300 MHz): δ (ppm) 6.40 (d; 2H), 6.15 (dd; 2H), 5.8 (d; 2H), 4.3 (t, 4H, $-\text{CH}_2$ a to acrylate ester) 3.75 (t, 4H, $-\text{CH}_2$ b to acrylate ester), 3.65 (s, 104H, CH_2 of PEG repeating units), 3.5 (57H, CH_2 of PPG repeat unit), 3.4 (28H, CH of PPG repeat unit), 1.15 (d, 110H, CH_3 of PPG repeating unit). IR (neat): abs cm^{-1} : 1730 ($\text{C}=\text{O}$ str), 810 ($\text{C}=\text{C}-\text{H}$ def), 1636 ($\text{C}=\text{C}$ str), 1109 ($\text{C}-\text{O}-\text{C}$ def), 2900 broad ($\text{C}-\text{H}$ str). GPC (THF, polystyrene standards): $M_n = 4360$, $M_w = 4870$, and $M_z = 5393$ g/mol.

Using this oligomer, a homogeneous formulation as given in Table 1 was prepared.

Results and Discussion

Real Time Dynamic Mechanical Analysis (RT-DMA). Figure 3a,b shows the shear stress and strain data vs time during UV cure of the acrylate formulation at 23 °C. The UV light is automatically switched on with a fixed delay of 1.575 s after start of the arbitrary wave experiment. Figure 3a shows the stress vs time and Figure 3b the applied strain vs time. The stress and strain signals display three apparent subcurves, which originate from the three samples that were taken per period of the sine wave. The sampling rate is too low to resolve the complete sine wave. Note that a minor misfit

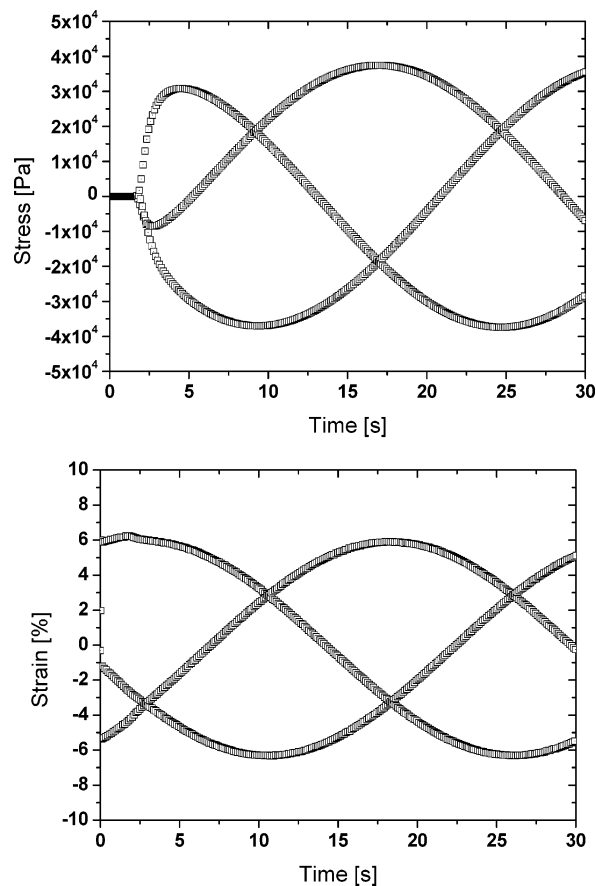


Figure 3. Stress (a) and strain (b) signals during the RT-DMA UV-cure experiment on the PPG acrylate formulation. UV illumination starts at $t = 1.575$ s.

between the frequency of the deformation sine wave and the sampling frequency results in a beat frequency with a period of about 64 s. This beat is removed by the subsequent Fourier analysis and has no significant

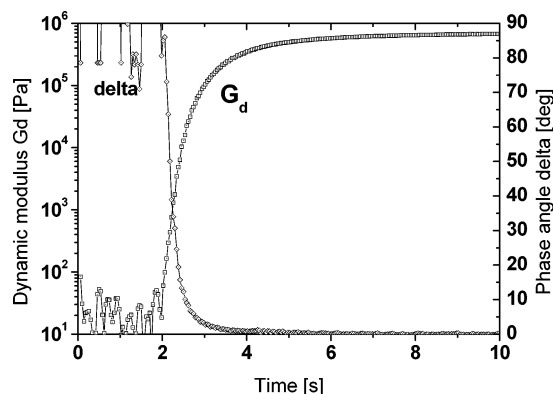


Figure 4. Dynamic modulus (G_d) on a logarithmic scale and the phase angle (δ), extracted with Fourier analysis from the stress and strain signals plotted against time in Figure 3. UV illumination starts at $t = 1.575$ s.

effect on the final results for the dynamic modulus and phase angle.

Initially, the stress shows no detectable signal. After about 2 s a sharp increase of the stress is observed, indicating a rise of the sample modulus. The dynamic modulus (G^*) and the phase angle (δ) were extracted via discrete Fourier transformation; the results are shown in Figure 4. The dynamic modulus is plotted along a logarithmic axis, which emphasizes the early time changes in the material, while the phase angle is plotted linearly along the right-hand y-axis.

At the start of the experiment the dynamic modulus of the material is too low (the viscosity is less than 1 Pa s) to be measured accurately with this instrument/geometry. At the same time, the phase angle shows large scatter around the theoretical value of 90° (Newtonian liquid) and cannot be accurately determined. Data reduction and smoothing was performed to remove extremely deviating data points and excessive noise. After about 2 s, the modulus starts to increase, and a drop of the phase angle is observed. Upon increase in modulus, the torque rises to within the range of the instrument, and the measured modulus and phase angle become accurate. The drop of the phase angle is indicative of the gel point; the liquid material transforms into an elastic rubbery solid. As the polymerization proceeds during further illumination, the shear modulus rises to a final value of about 700 kPa.

Real Time Near-Infrared Spectroscopy (RT-NIRS). In the monitoring of the acrylate group, no distinction is made between the monofunctional acrylate of ENPA and the oligomeric PPG diacrylate though it is recognized that these two types of acrylate will have different reactivities as indicated by Bowman.²³ However, in these fast bulk acrylate photopolymerizations it is not possible to distinguish between the oligomer- and monomer-based acrylates by either mid-infrared or near-infrared spectroscopy.

Figure 5 clearly reveals the time-dependent disappearance of the acrylate peak (indicated by an arrow). All measured spectra exhibit a shift to negative absorption values. This is attributed to slight changes in reflectance within the measurement cell after loading the sample material (glass/sample vs glass/air interface) and shrinkage. The UV lamp when switched on has an infrared emission that affects the baseline. The baseline drifts slightly during the measurements. All these effects can be compensated for with appropriate spectral data processing techniques.

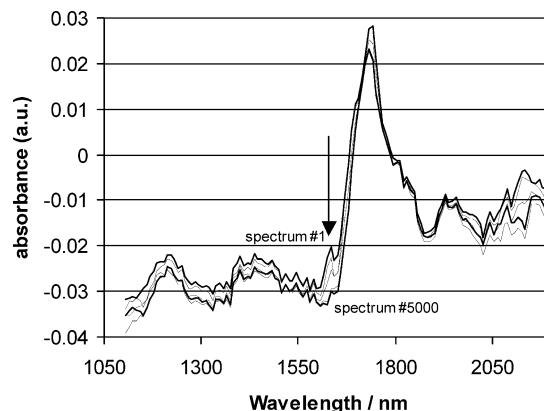


Figure 5. Acrylate polymerization at 1617 nm shown with a selection of NIR spectra collected during the UV polymerization cure of the PPG acrylate/DEGEHA formulation.

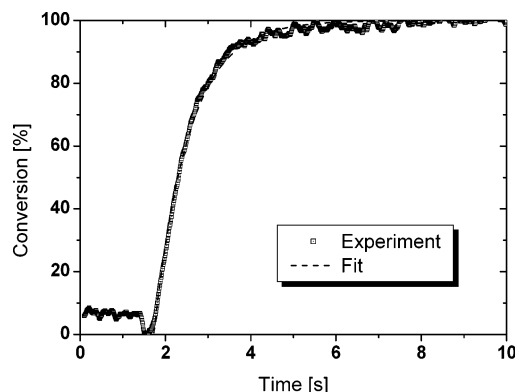


Figure 6. Unsaturated bond conversion of the PPG3100-diacrylate/ENPA formulation as a function of time during the UV exposure, measured by RT-NIR spectroscopy at 1617 nm. The dashed line shows the fit of the experimental data to the steady-state reaction kinetics model. UV illumination starts at $t = 1.575$ s. Error in conversion $\pm 2.0\%$

Figure 6 shows the acrylate conversion at 1617 nm, extracted from the RT-NIR cure scan. About 0.2 s before the increase of the dynamic modulus (see Figure 4), the acrylate conversion starts to increase. The apparent drop in the conversion at the moment that the UV illumination is switched on is attributed to an interference of NIR fluorescence emitted by the sample with the actual NIR measurement. It was corrected for by renormalization of the data.

The profiles of conversion p vs time (t) were fitted with a simple n th-order steady-state reaction kinetics model. It is acknowledged that steady-state reaction kinetics oversimplify the actual kinetics; however, we did obtain a good description of the experimental curves with the steady-state equations:

$$p(t) = 1 - \frac{1}{[1 + (n-1)k(T)(t-t_0)]^{1/(n-1)}} \quad \text{for } n > 1 \quad (1)$$

and

$$p(t) = 1 - \exp(-k(T)(t-t_0)) \quad \text{for } n = 1 \quad (2)$$

in which $k(T)$ [s^{-1}] is the temperature-dependent reaction rate constant, n ($n > 1$) the reaction order, and t_0 a time shift correcting for the delay between the start of the near-IR measurement and UV illumination. The dashed line in Figure 6 shows the best fit of eq 1 to the

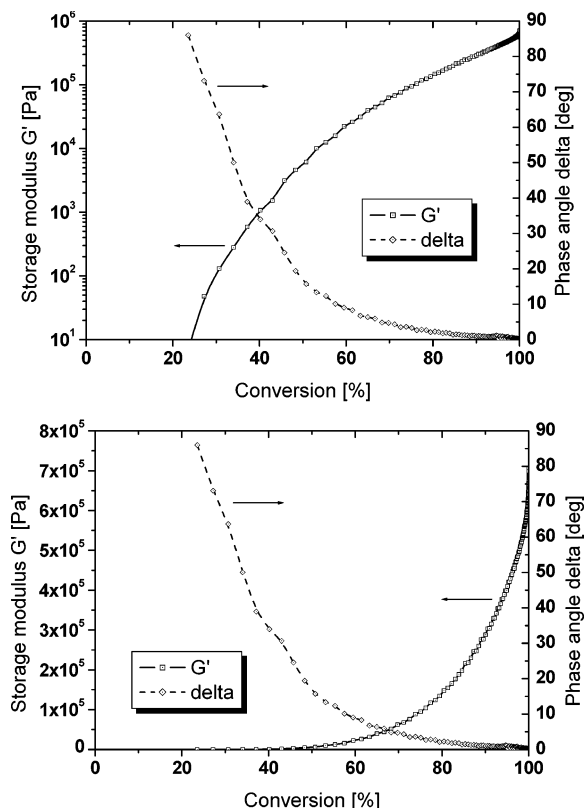


Figure 7. Dynamic modulus and the phase angle as a function of the unsaturated bond conversion of the PPG acrylate formulation during the UV-cure experiment in logarithmic (a) and linear (b) presentation.

experimental data. The reaction order was found to be $n = 1.0 \pm 0.05$, while the rate constant k amounts to $1.23 \pm 0.05 \text{ s}^{-1}$.

Network Formation in Relation to Chemical Conversion. The common practice in understanding development of mechanical properties during UV cure is the plotting of so-called dose–modulus curves, i.e., the modulus vs the applied UV dose. This approach is useful to monitor development of properties with UV dose but is of less utility to understand the relation between chemical conversion and mechanical properties of a particular formulation in a time-resolved manner. In contrast, the RT-DMA/NIRS results allow plotting of chemical conversion vs modulus curves during the course of the reaction. These curves yield valuable information for design and optimization of photocurable materials.

Figure 7a,b shows a plot of the dynamic mechanical properties vs the acrylate conversion. In these graphs the storage modulus $G' = G^* \cos(\delta)$ was plotted instead of the dynamic modulus G^* since this property reflects the formation of an elastically active network more sensitively. Figure 7a shows the modulus along a logarithmic axis, while Figure 7b is a linear presentation of the same data. Until 20% acrylate conversion, the elastic modulus of the material is too low to be measured accurately. Phase angle data showing large scatter were removed from the plot. Above 20% acrylate conversion, the phase angle drops sharply with increasing conversion, and a nonzero elastic modulus is detected. At about 35% acrylate conversion the phase angle drops below 45° . This point is often referred to as the gel point since it indicates the moment when the behavior of the material changes from mainly liquidlike to solidlike. Use

of the Winter–Chambon criterion to detect the gel point, as done by Kahn,¹¹ would have been more appropriate but was not possible since only a single measurement frequency was available. Above 60% conversion, the dynamic modulus becomes visible on the linear scale used in Figure 7b and increases exponentially until complete acrylate conversion. Figure 7b clearly reveals that the major part of the network formation, development of modulus, occurs above 90% conversion for this particular formulation.

Khan et al. were able to make a similar plot of modulus version conversion by combining the results of separately performed (at identical light intensity) real time infrared and real time dynamic mechanical experiments.¹² They were able to make this combination of results because of the much longer time scale (typical 1000 s) of their experiments, which makes slight differences in timing not very critical. On the time scale of acrylic photopolymerizations (typically 1–10 s) this would be impossible, and use of a hyphenated technique is absolutely required. Our results of modulus vs conversion with radical acrylate chain growth polymerization are similar to results of the thiol–ene step growth photopolymerization experiments performed by Khan.¹² The most striking difference is the conversion at which the first indications of the presence of an elastically active network is detected, which occurs in the acrylic case (chain growth polymerization) at a conversion of about 20%, while in the thiol–ene case (step-growth polymerization) this occurs at about 65% reactive group conversion.

Finally, we want to draw attention to the fact that a significant fraction of the final network density is developed at conversions above 98%, which is at the limits of accuracy with infrared spectroscopy. This emphasizes the importance in getting as complete a chemical conversion as possible so as to achieve the desired properties; i.e., the systems are very sensitive to incomplete acrylate conversion. This observation brings into question the merit of the use of the maximum rate of polymerization^{1,2} (R_p) as determined spectroscopically at low acrylate conversions (e.g., with IR) as a measurement of cure speed. It suggests that if one considers cure in terms of the development of mechanical properties, more attention should be given to the time to achieve high acrylate conversion rather than the maximum rate of polymerization.¹

Conclusions

Network formation (modulus buildup) during photopolymerization has been monitored in real time with simultaneous measurement of polymerization (acrylate bond consumption). This has been achieved by coupling of rapid scan, diode array, near-infrared spectroscopy with real time dynamic mechanical analysis. Through high data acquisition rates, fast cross-linking polymerizations can be followed. The dynamic mechanical measurements have a resolution of up to 50 data points/s, while the spectroscopic measurements have a resolution of up to 374 spectra/s. This experimental setup is suitable for materials with a final shear modulus up to approximately 10 MPa.

In an example with a PPG-based acrylate formulation this hyphenated technique has clearly revealed that a distinction has to be made between the conventional spectroscopic approach to measure polymerization speed in terms of reactive group conversion and cure speed in

terms of network formation toward development of mechanical properties. While the maximum rate of polymerization (R_p) is important, more attention should be focused on the ultimate level of conversion when one acknowledges the dramatic effect it has on the network structure and ultimately the mechanical properties.

A better understanding of network formation by this new RT-DMA/NIRS technique will help in designing new high-performance photocurable coatings. This technique can be used to examine all manner of cross-linking photopolymerizations ranging from free radical acrylate homopolymerizations and maleate vinyl ether copolymerizations to step growth polymerizations (thiol-ene) as well as cationic and anionic photopolymerizations.

Acknowledgment. The authors thank Erwin Houben, Robbert van Sluijs, Ton Sleijpen, Jo Palmen, and Marnix Rooijmans, all from DSM Research, for their contributions to this work. We thank in particular Huub van Cleef, who designed and made the tailor-made parallel plate geometry and holder in-house. Finally, we thank the management of DSM Desotech for their support and permission to publish this work.

References and Notes

- (1) Decker, C.; Moussa, K. *Makromol. Chem.* **1988**, *189*, 2381.
- (2) Dias, A. A.; Hartwig, H.; Jansen, J. F. G. A. *Surf. Coat. Int., JOCCA* **2000**, *8*, 382.
- (3) Lin, Y.; Stansbury, J. *ACS Polym. Prepr.* **2001**, *42* (2), 809.
- (4) Nelson, E. W.; Scranton, A. B. *Polym. Mater. Sci. Eng.* **1995**, *72*, 413.
- (5) Carlini, C.; Rolla, P. A.; Tombari, E. *J. Polym. Sci., Polym. Phys.* **1989**, *27*, 189.
- (6) Carlini, C.; Rolla, P. A.; Tombari, E. *J. Appl. Polym. Sci.* **1990**, *41*, 805–818.
- (7) Nakamuchi, T. *Prog. Org. Coat.* **1986**, *14*, 23.
- (8) Watanabe, K.; Amari, T.; Otsubo, Y. *J. Appl. Polym. Sci.* **1984**, *29*, 57.
- (9) Davison, J.; Guthrie, J. T. *Surf. Coat. Int., JOCCA* **1992**, *75*, 316.
- (10) Ottersbach, P.; Lennarz, K.; Bargon, J. *Makromol. Chem. Phys.* **1994**, *195*, 3929.
- (11) Chiou, B.-S.; English, R.; Khan, S. A. *Macromolecules* **1996**, *29*, 5368.
- (12) Chiou, B.-S.; Khan, S. A. *Macromolecules* **1997**, *30*, 7322.
- (13) Flory, P. J. *Principles of Polymer Chemistry*; Cornell University Press: Ithaca, NY, 1953; Chapter IX.
- (14) Stockmayer, W. H. *J. Chem. Phys.* **1943**, *11*, 45.
- (15) Stockmayer, W. H. *J. Chem. Phys.* **1944**, *12*, 125.
- (16) Gordon, M. *Proc. R. Soc. London, Ser. A* **1962**, *268*, 240.
- (17) Macosko, C. W.; Miller, D. R. *Macromolecules* **1976**, *9*, 206.
- (18) Durand, D.; Bruneau, C.-M. *Eur. Polym. J.* **1985**, *21*, 527–535, 611.
- (19) Tobita, H.; Hamielec, A. *Makromol. Chem. Macromol. Symp.* **1988**, *20/21*, 501.
- (20) Mikos, A. G.; Takoudis, C. G.; Peppas, N. A. *Macromolecules* **1986**, *19*, 2174.
- (21) Boots, H. M. J.; Kloosterboer, J. G.; Hei van de, G. M. M. *Br. Polym. J.* **1985**, *17*, 219.
- (22) Anseth, K. A.; Bowman, C. N. *Chem. Eng. Sci.* **1994**, *49*, 2207.
- (23) Elliot, J. E.; Bowman, C. N. *Macromolecules* **2001**, *34*, 4642.

MA049366C